

Dispersion Relation for the Nucleon Electromagnetic Form Factors

Susumu FURUICHI*

Department of Physics, Rikkyo University, Toshima Tokyo 171-8501, Japan

Hirohisa ISHIKAWA†

Department of Economy, Meikai University, Urayasu Chiba, 279-8550, Japan

Keiji WATANABE‡

Department of Physics, Meisei University, Hino Tokyo 191-8506, Japan

Abstract

Elastic electromagnetic form factors of nucleons are investigated both for the time-like and the space-like momentums by using the unsubtracted dispersion relation with QCD constraints. It is shown that the calculated form factors reproduce the experimental data reasonably well; they agree with recent experimental data for the neutron magnetic form factors for the space-like data obtained by the CLAS collaboration and are compatible with the ratio of the electric and magnetic form factors for the time-like momentum obtained by the BABAR collaboration.x

PACS No. 13.40.Gp, 12.38.-tm, 11.55.Fv

1 Introduction

Recently, there are remarkable developments in experiments for the nucleon electromagnetic form factors:

1) For the space-like momentum, the ratio of the electric and magnetic form factors of proton, G_E^p and G_M^p respectively, was shown to be a decreasing function of the squared momentum transfer Q^2 and the experimental results imply that the proton electric form factor vanishes for $Q^2 \approx 7(\text{GeV}/c)^2$ [1]-[5].

2) For the neutron magnetic form factor, G_M^n , very accurate experimental data were obtained and it approximately satisfies $G_M^n(Q^2)/\mu_n \approx G_D(Q^2) = (1 + Q^2/0.71)^{-2}$, with Q being represented in terms of GeV/c , for fairly wide range of squared momentum transfer $Q^2 = 1.4 - 4.8 (\text{GeV}/c)^2$ [6], [7] (CLAS collaboration).

*Mailing address: Sengencho 3-2-6, Higashikurume Tokyo 203-0012

†e-mail address: ishikawa@meikai.ac.jp

‡e-mail address keijiwatanabe888@yahoo.co.jp; Mailing address: Akazutumi, 5-36-2, Setagaya Tokyo 156-0044

3) For the time-like momentum the ratio $|G_E^p/G_M^p|$ was obtained [8], [9] (BABAR collaboration), while previously the data of form factors had been analyzed under the assumption $G_E^p = 0$ or $G_E^p = G_M^p$.

Asymptotically, the experimental data of nucleon magnetic factors decrease more rapidly than the dipole formula for large Q^2 and the decrease has been understood as a realization of perturbative QCD [10], the behavior of which can be formulated in terms of the dispersion theory with appropriate conditions on the absorptive parts; we assumed unsubtracted dispersion relations for the charge and magnetic moment form factors. To realize the asymptotic form of QCD we imposed the superconvergence conditions.

As the data for the time-like momentum have become accurate, it is necessary to investigate the form factors for the space-like and time-like momentums systematically. For this purpose the dispersion theory is effective.

The dispersion theoretical calculations performed so far, the value of G_M^n turned out to be larger than the above mentioned new experimental data for $Q^2 = 1.4 - 4.8$ (GeV/c)² (see Ref. [7]). It is of vital importance to investigate if it is possible to realize the experimental data simply by the adjustment of parameters or by the refinement of absorptive parts in the dispersion relation.

It is the purpose of this paper to analyze experimental data of nucleon form factors by the dispersion theory, with the QCD constraints imposed, taking account of the above mentioned new experimental results.

Organization of the paper is given as follows: In Sec. 2 we explain the superconvergent dispersion relation and give conditions which are used in this paper. We summarize the absorptive parts, which are broken up into three parts: Low, intermediate and asymptotic momentum regions. For each momentum region the imaginary parts are given. The asymptotic part is expressed as an expansion in terms of the analytically regularized running coupling constant in the renormalization group for QCD. In Sec. 3 we remark on the numerical analysis. In Sec. 4 numerical results are summarized. The final section is devoted to general discussions.

2 Dispersion Relation for the Electromagnetic Form Factors

We assume the unsubtracted dispersion relations for the charge and magnetic moment form factors, F_1^I and F_2^I , respectively, with I denoting the isospin state $I = 0, 1$. That is,

$$F_i^I = \frac{1}{\pi} \int_{t_0}^{\infty} dt' \frac{\text{Im} F_i^I(t')}{t' - t}, \quad (i = 1, 2) \quad (1)$$

where the threshold is $t_0 = 4\mu^2$. Here μ is the pion mass being taken as the average of the neutral and charged pion masses. We impose conditions on $\text{Im} F_i^I$ to realize the QCD conditions.

2.1 Superconvergence Condition and QCD

Experimental data imply that the magnetic form factors of nucleon decrease more rapidly than the dipole formula for large squared momentum transfer. The decrease agrees with the prediction of perturbative QCD, where magnetic form factors of nucleon decrease for $Q^2 \rightarrow \infty$ as

$$G_M(q^2) \rightarrow \text{const} \frac{\alpha_S(Q^2)^2}{Q^4} \left(\ln \frac{Q^2}{\Lambda^2} \right)^{4/3\beta_0}, \quad (2)$$

where α_S is the running coupling constant of QCD and $\beta_0 = 11 - 2n_f/3$ with n_f being the number of flavor. Λ is the QCD scale parameter having the dimension of momentum.

To realize the QCD predictions we impose the following conditions on the charge and magnetic moment form factors:

$$\begin{aligned} F_1(Q^2) &\rightarrow \text{const}/[Q^2(\ln Q^2/\Lambda^2)^\gamma], \\ F_2(Q^2) &\rightarrow \text{const}/[Q^4(\ln Q^2/\Lambda^2)^\gamma], \end{aligned} \quad (3)$$

for $Q^2 \rightarrow \infty$ with $\gamma \geq 2$.

We briefly summarize the asymptotic theorems which are used to incorporate the constraints of QCD [10], where the proof is given in Ref. [18]. Let $F(t)$ satisfy the dispersion relation (1), and $\text{Im}F$ is given as

$$\text{Im}F(t') = \frac{c}{[\ln(t'/\Lambda^2)]^{\gamma+1}} + O\left(\frac{1}{[\ln(t'/\Lambda^2)]^{\gamma+2}}\right) \quad (4)$$

for $t \rightarrow \infty$ with $\gamma > 1$. Then $F(t)$ becomes

$$\begin{aligned} F(t) &= \frac{1}{\pi} \int_{t_0}^{\infty} dt' \frac{c}{(t' - t)[\ln(t'/\Lambda^2)]^{\gamma+1}} \\ &\rightarrow \frac{c}{\pi\gamma \ln(|t|/\Lambda^2)^\gamma} \end{aligned} \quad (5)$$

for $t \rightarrow \pm\infty$. Generally, when $F(t')$ satisfies

$$t'^{n+1} \text{Im}F(t') \rightarrow \frac{c}{[\ln(t'/\Lambda^2)]^{\gamma+1}} + O\left(\frac{1}{[\ln(t'/\Lambda^2)]^{\gamma+2}}\right) \quad (6)$$

for $t' \rightarrow \infty$ and the superconvergence conditions

$$\int_{t_0}^{\infty} dt' t'^k \text{Im}F(t') = 0, \quad k = 0, 1, \dots, n, \quad (7)$$

$F(t)$ given by (1) approaches for $t \rightarrow \pm\infty$ to the following formula:

$$F(t) = \frac{1}{\pi} \int_{t_0}^{\infty} dt' \frac{\text{Im}F(t')}{t' - t} \rightarrow \frac{1}{t^{n+1}} \frac{c}{\pi\gamma [\ln(|t|/\Lambda^2)^\gamma]}, \quad (8)$$

which can be proved by using (6) and (7) together with the identity

$$\frac{1}{t' - t} = -\frac{1}{t} \left\{ 1 + \frac{t'}{t} + \dots + \left(\frac{t'}{t}\right)^n \right\} + \frac{1}{t^{n+1}} \frac{t'^{n+1}}{t' - t}.$$

Indeed, by using (7) we have

$$\int_{t_0}^{\infty} dt' \frac{\text{Im}F(t')}{t' - t} = \frac{1}{t^{n+1}} \int_{t_0}^{\infty} dt' \frac{t'^{n+1} \text{Im}F(t')}{t' - t}, \quad (9)$$

which leads to (8) as $t'^{n+1} \text{Im}F(t')$ satisfies (6).

To obtain the asymptotic formulas (3), therefore, we impose the superconvergence conditions on the imaginary part of form factors, $\text{Im}F_i^I(t)$ ($i = 1, 2$; I denotes isospin) in the unsubtracted dispersion relation (1):

$$\begin{aligned} \frac{1}{\pi} \int_{t_0}^{\infty} dt' \text{Im}F_1^I(t') &= \frac{1}{\pi} \int_{t_0}^{\infty} dt' t' \text{Im}F_1^I(t') = 0, \\ \frac{1}{\pi} \int_{t_0}^{\infty} dt' \text{Im}F_2^I(t') &= \frac{1}{\pi} \int_{t_0}^{\infty} dt' t' \text{Im}F_2^I(t') = \frac{1}{\pi} \int_{t_0}^{\infty} dt' t'^2 \text{Im}F_2^I(t') = 0, \end{aligned} \quad (10)$$

where $\text{Im}F_i^I(t')$ satisfies the asymptotic conditions for $t' \rightarrow \infty$

$$t'^i \text{Im}F_i^I(t') \rightarrow \text{const}/[\ln(t'/\Lambda^2)]^{\gamma+1} \quad (i = 1, 2). \quad (11)$$

In addition to the conditions (10) and (11) we impose the normalization conditions at $t = 0$:

$$\frac{1}{2} = \frac{1}{\pi} \int_{t_0}^{\infty} dt' \text{Im}F_1^I(t')/t', \quad (12)$$

$$g^I = \frac{1}{\pi} \int_{t_0}^{\infty} dt' \text{Im}F_2^I(t')/t', \quad (13)$$

where g^I is the anomalous magnetic moments of nucleons with the isospin I .

2.2 Imaginary part of the form factors

Let us discuss the imaginary parts of nucleon form factors, which are broken up into three parts: The low momentum, the intermediate, and the asymptotic regions.

2.2.1 Low momentum region

The imaginary parts of the charge and magnetic moment form factors, $\text{Im}F_i^V$, are given in terms of two pion contribution as follows:

$$\begin{aligned} \text{Im}[F_1^V(t)/e] &= \frac{m}{2} \frac{(t-4\mu^2)}{4m^2-t} \left(\frac{t-4\mu^2}{t} \right)^{1/2} \\ &\times \text{Re} \left[M^*(t) \left\{ f_+^{(-)1}(t) - \frac{t}{4m^2} \frac{m}{\sqrt{2}} f_-^{(-)1}(t) \right\} \right], \\ \text{Im}[2mF_2^V(t)/e] &= \frac{m}{2} \frac{(t-4\mu^2)}{(4m^2-t)} \left(\frac{t-4\mu^2}{t} \right)^{1/2} \\ &\times \text{Re} \left[M^* \left\{ \frac{m}{\sqrt{2}} f_-^{(-)1}(t) - f_+^{(-)1}(t) \right\} \right], \end{aligned} \quad (14)$$

where $f_{\pm}^{(-)1}(t)$ are helicity amplitudes for $\pi\pi \leftrightarrow N\bar{N}$, $M(t)$ is the pion form factor and μ is the pion mass. The superscript V denotes the iso-vector part. For the helicity amplitudes we use the numerical values given by Höhler and Schopper [16] and parameterize $M(t)$ according to them.

$$M(t) = t_{\rho} \{ 1 + (\Gamma_{\rho}/m_{\rho}d) \} [t_{\rho} - t - im_{\rho}^2 \Gamma_{\rho} (q_t/q_{\rho})^3 \sqrt{t}]^{-1}, \quad (15)$$

where m_{ρ} and Γ_{ρ} are the ρ meson mass and width respectively and

$$t_{\rho} = m_{\rho}^2, \quad q_{\rho} = \sqrt{t_{\rho} - \mu^2}, \quad (16)$$

$$d = \frac{3\mu^2}{\pi t_{\rho}} \ln \frac{m_{\rho} + 2q_{\rho}}{2\mu} + \frac{m_{\rho}}{2\pi q_{\rho}} \left(1 - \frac{2\mu^2}{t_{\rho}} \right). \quad (17)$$

The imaginary parts thus obtained are denoted as $\text{Im}F_i^H$ ($i = 1, 2$) hereafter. It must be remarked that the ρ meson contribution is included in the helicity amplitudes of Ref. [16]. The uncorrelated kaon pair is neglected here as the effect was estimated to be small [17].

2.2.2 Intermediate region

The intermediate states $4\mu^2 \leq t \leq \Lambda_1^2$ are approximated by the addition of the Breit-Wigner terms, with the imaginary part parameterized as follow:

$$\text{Im}f_R^{BW}(t) = \frac{g}{(t - M_R^2)^2 + g^2}, \quad (18)$$

where

$$g = \frac{\Gamma M_R^2 (M_R^2 + t_{res})^3}{t_{res}^2 (M_R^2 - t_0)^{3/2}} \sqrt{\frac{(t - t_0)^3}{t}} \frac{t^2}{(t + t_{res})^3}. \quad (19)$$

Here M_R and Γ are the mass and width of resonance, respectively, the threshold t_0 is $t_0 = 4\mu^2$ and t_{res} is treated as an adjustable parameter. g is introduced to cut-off the Breit-Wigner formula.

We write the intermediate part as the summation of resonances

$$\text{Im}F_i^{BW,I} = \sum_n a_n^{I,i} f_{nR}^I, \quad (20)$$

where I is the isospin and n is the labeling of resonances (see Table I). Here the suffix i denotes $i = 1, 2$, corresponding to the charge and magnetic moment form factors F_1^N and F_2^N ($N = n$ or p). The same formulas for f_{nR}^I are used for $i = 1$ and $i = 2$.

2.2.3 Asymptotic region

We express the form factors as power series in the running coupling constant of QCD, α_S . To calculate the absorptive part, it is necessary to perform analytic continuation to the time-like momentum. Here we give only the necessary procedure for the analytic continuation of the running coupling constant to the time-like momentum by using the analytic regularization [12] [13], as the formulation is given in Ref. [18].

Let $\alpha_S(Q^2)$ be the running coupling constant in the renormalization group calculated by the perturbative QCD as the function of the squared momentum Q^2 for the space-like momentum. We use the three loop approximation for $\alpha_S(Q^2)$, which is expressed in the Padé form.

$$\alpha_S(Q^2) = \frac{4\pi}{\beta_0} \left[\ln(Q^2/\Lambda^2) + a_1 \ln\{\ln(Q^2/\Lambda^2)\} + a_2 \frac{\ln\{\ln(Q^2/\Lambda^2)\}}{\ln(Q^2/\Lambda^2)} + \frac{a_3}{\ln(Q^2/\Lambda^2)} + \dots \right]^{-1}. \quad (21)$$

Λ is the QCD scale parameter, and a_i are expressed in terms of the β function of QCD,

$$a_1 = 2\beta_1/\beta_0^2, \quad a_2 = 4\frac{\beta_1^2}{\beta_0^4}, \quad a_3 = \frac{4\beta_1^2}{\beta_0^4} \left(1 - \frac{\beta_0\beta_2}{8\beta_1^2} \right), \quad (22)$$

where

$$\beta_0 = 11 - \frac{2n_f}{3}, \quad \beta_1 = 51 - \frac{19n_f}{3}, \quad \beta_2 = 2357 - \frac{5033}{9}n_f + \frac{325}{27}n_f^2 \quad (23)$$

with n_f being the number of flavor. We perform the analytic continuation of the squared momentum to the time-like region, s , by the replacement in (21)

$$Q^2 \rightarrow e^{-i\pi} s. \quad (24)$$

Then $\alpha_S(e^{-i\pi} s)$ becomes complex and is expressed as follows:

$$\alpha_S(e^{-i\pi} s) = 1/(u - iv) = \frac{u + iv}{D}, \quad (25)$$

$$D = u^2 + v^2, \quad (26)$$

where u and v are given as

$$\begin{aligned}
u &= \ln(s/\Lambda^2) + \frac{a_1}{2} \ln\{\ln^2(s/\Lambda^2) + \pi^2\} \\
&+ \frac{a_2}{\ln^2(s/\Lambda^2) + \pi^2} \left[\frac{1}{2} \ln(s/\Lambda^2) \ln\{\ln^2(s/\Lambda^2) + \pi^2\} \right] \\
&+ \frac{a_3 \ln(s/\Lambda^2)}{\ln^2(s/\Lambda^2) + \pi^2},
\end{aligned} \tag{27}$$

$$\begin{aligned}
v &= \pi + a_1 \theta \\
&- \frac{a_2}{\ln^2(s/\Lambda^2) + \pi^2} \left[\frac{\pi}{2} \ln\{\ln^2(s/\Lambda^2) + \pi^2\} - \theta \ln(s/\Lambda^2) \right] \\
&- \frac{\pi a_3}{\ln\{\ln^2(s/\Lambda^2) + \pi^2\}},
\end{aligned} \tag{28}$$

with

$$\theta = \tan^{-1}\{\pi/\ln(s/\Lambda^2)\}. \tag{29}$$

The running coupling constant is given by the dispersion integral both for the space-like and the time-like momentum

$$\alpha_R(t) = \int_0^\infty dt' \frac{\sigma(t')}{t' - t} \tag{30}$$

with

$$\sigma(t') = \text{Im}\alpha_S(e^{-i\pi}s) = 4\pi v/\beta_0 D. \tag{31}$$

$\alpha_R(t)$ represented by (30) is called analytically regularized running coupling constant as it has no singular point for $t = -Q^2 < 0$. The regularization eliminates the ghost pole of $\alpha_S(Q^2)$, given by (21), appearing at

$$Q^2 = \bar{Q}^{*2} = \Lambda^2 e^{u^*}, \tag{32}$$

where $u^* = 0.7659596 \dots$ for the number of flavor $n_f = 3$. Calculating (30), we find that $\alpha_R(t)$ is approximately given by the simple formula with the ghost pole subtracted

$$\alpha_R(Q^2) \approx \alpha_S(Q^2) - A^*/(Q^2 - \bar{Q}^{*2}), \tag{33}$$

where the residue A^* is

$$A^* = 4\pi\Lambda^2 e^{u^*} / \left\{ \beta_0 \left(1 + \frac{a_1}{u^*} - a_2 \frac{\ln u^*}{u^{*2}} + \frac{a_2 - a_1}{u^{*2}} \right) \right\}. \tag{34}$$

We use (33) as the regularized coupling constant; for the time-like momentum we replace $Q^2 \rightarrow e^{-i\pi}s$ in (33) as was mentioned before.

The QCD parts, $F_i^{QCD,I}$ ($i = 1, 2; I = 0, 1$) for the squared time-like momentum, are written as follows:

$$F_i^{QCD,I}(s) = \hat{F}_i^{QCD,I}(s) h_i(s), \tag{35}$$

where $\hat{F}_i^{QCD,I}$'s are given as expansion in terms of the running coupling constant

$$\hat{F}_i^{QCD,I}(s) = \sum_{j \geq 2} c_j^{QCD,I} \{\alpha_R(s)\}^j \tag{36}$$

for the time-like squared momentum s . We multiply by the function $h(s)$ in (35) to assure the convergence of the superconvergence conditions (10) and (11). The following formula is assumed for $h_i(s)$:

$$h_i(s) = \left(\frac{s - t_Q}{s + t_1} \right)^{3/2} \left(\frac{t_2}{s + t_2} \right)^{i+1}, \quad (37)$$

which may be interpreted as the form factor for $\gamma \rightarrow q\bar{q}$ with t_Q being the threshold of the quark antiquark pair. The parameters t_Q , t_1 and t_2 are taken as adjustable parameters and will be determined by the analysis of experimental data.

For the time-like momentum, we perform the analytic continuation of the regularized effective coupling constant $\alpha_R(Q^2)$ to $\alpha_R(s)$ through the equation

$$\alpha_R(s) = \alpha_R(Q^2 e^{-i\pi}) = \text{Re}[\alpha_R(s)] + i \text{Im}[\alpha_R(s)]. \quad (38)$$

We express the QCD part as the power series expansion in $\alpha_R(s)$

$$\hat{F}_i^{QCD,I}(s) = \sum_{2 \leq j} c_{i,j}^{QCD,I} \{\alpha_R(s)\}^j. \quad (39)$$

The summation in (39) begins in the second order in the effective coupling constant so as to realize the logarithmic decrease of the nucleon form factors.

Imaginary part of (39) is obtained to be

$$\begin{aligned} \text{Im} \hat{F}_i^{QCD,I} &= 2c_{i,2}^{QCD,I} \text{Re} \alpha_R \text{Im} \alpha_R \\ &+ c_{i,3}^{QCD,I} [3(\text{Re} \alpha_R)^2 \text{Im} \alpha_R - (\text{Im} \alpha_R)^3] \\ &+ c_{i,4}^{QCD,I} [4(\text{Re} \alpha_R)^3 \text{Im} \alpha_R - 4\text{Re} \alpha_R (\text{Im} \alpha_R)^3] \\ &+ \dots, \end{aligned} \quad (40)$$

and

$$\text{Im} F_i^{QCD,I}(s) = \text{Im} \hat{F}_i^{QCD,I}(s) h_i(s). \quad (41)$$

We write the low energy part, intermediate resonance part and asymptotic QCD parts of form factors as F_i^H , $F_i^{BW,I}$ and $F_i^{QCD,I}$, respectively, which are given by the dispersion integral with the imaginary parts (14), (20) and (41). The form factors F_i^I are defined by adding them up. We impose the conditions (10) and (11) on $\text{Im} F_i^I$ so that the QCD conditions are satisfied.

3 Numerical Analysis

We analyzed the experimental data of nucleon electromagnetic form factors $G_M^p/\mu_p G_D$, G_E^p/G_D , $G_M^n/\mu_n G_D$, G_E^n and the ratio $\mu_p G_E^p/G_M^p$ for the space-like momentum transfer, and $|G^p|$ and $|G^n|$ in Refs. [19]- [40] for the time-like momentum transfer and the above mentioned recent experimental data G_M^n for the space-like and $|G_E^p/\mu_p G_M^p|$ for the time-like momentum transfer. The parameters appearing in the formulas are determined so as to minimize χ^2 .

As was mentioned in the introduction we analyze by taking account of the recent experimental data: (a) G_M^n for $Q^2 = 1 - 4.8$ (GeV/c)² (CLAS collaboration) and (b) $|\mu_p G_E^p|/|G_M^p|$ (BABAR collaboration).

In order to see how the situation changes by taking account of these new experiments in addition to the other data, we perform analysis for the following two cases in the χ^2 analysis:

Case I: Both of the experimental data, (a) $|\mu_p G_E^p/G_M^p|$ for the time-like momentum and (b) new data for G_M^n for the space-like momentum, are added.

Case II: Only the data (a) $|\mu_p G_E^p/G_M^p|$ for the time-like momentum are added.

Let us remark on the experiments for the time-like momentum [8], [32], [33], where the form factors $|G^p|$ and $|G^n|$ are determined by using the formula for the cross section σ_0 for the processes $e + \bar{e} \rightarrow N + \bar{N}$ or $N + \bar{N} \rightarrow e + \bar{e}$, which is given as

$$\sigma_0 = \frac{4\pi\alpha^2\nu}{3s} \left(1 + \frac{2m_p^2}{s} \right) |G(s)|^2. \quad (42)$$

Here α is the fine structure constant and ν is the nucleon velocity. $|G_M^N|$ are estimated from $|G|$ under the assumption $G_M = G_E$ or $G_E = 0$. σ_0 is expressed in terms of G_M^N and G_E^N as follows:

$$\sigma_0 = \frac{4\pi\alpha^2\nu}{3s} \left(|G_M^N|^2 + \frac{2m^2}{s} |G_E^N|^2 \right). \quad (43)$$

Equating (42) and (43), we have

$$|G|^2 = \frac{|G_M^N|^2 + 2m^2|G_E^N|^2/s}{1 + 2m^2/s}. \quad (44)$$

Substituting our calculated result of form factors to the right hand side of (44), we obtain the theoretical value for $|G|$, which is compared with the experimental data for the magnetic form factor obtained under the assumption $G_M = G_E$.

The parameters appearing in our analysis are the following: Residues at resonances, coefficients appearing in the expansion by the QCD effective coupling constants, cut-offs for the intermediate region Λ_1 . In addition to them we have parameters in the Breit-Wigner formula and the convergence factor h of QCD contribution, t_Q , t_{res} , t_1 , t_2 , t_3 .

We have taken the masses and the widths of resonances as adjustable parameters. As the superconvergence constraints impose very stringent conditions on the form factors, it was necessary to take the masses and widths as parameters.

4 Numerical Results

We give in Tables 1, 2 and 3 the results for the parameters for the cases I and II obtained by the χ^2 analysis; in Table 1 the masses and widths of resonances and in Table 2 residues at resonance poles and in Table 3 the coefficients $c_{i,j}^{QCD,I}$ ($i = 1, 2$; $j = 2, 3, 4$; $I = 0, 1$) in the expansion in terms of the effective coupling constant α_R of QCD defined by (39). The number of flavor is taken as $n_f = 3$. $\text{Im}F_i^H$ is cut-off at $\Lambda_0^2 = 0.779 \text{ GeV}^2$ and the Breit-Wigner formulas at $\Lambda_1 = 26.0 \text{ GeV}$. The QCD parameter is fixed at $\Lambda = 0.216 \text{ GeV}$. The other parameters are determined as follows: Case I: $t_0 = 4\mu^2$, $t_1 = 0.243 \times 10^3 \text{ GeV}^2$, $t_2 = 0.237 \times 10^3 \text{ GeV}^2$, $t_{res} = 0.2260 \times 10^3 \text{ GeV}^2$, $t_Q = 0.202 \times 10^2 \text{ GeV}^2$.

Case II: The same as in the case I except for $t_{res} = 0.2253 \times 10^3 \text{ GeV}^2$.

The value of χ^2 is obtained to be $\chi_{tot}^2 = 393.4$ for the case I and $\chi_{tot}^2 = 308.7$ for the case II, which includes both the data of space-like and time-like regions. The total number of data is 245 for the Case I and 236 for the Case II. Number of parameters is 36 so that $\text{DOF}/\chi_{min} = 1.88$ for the Case I and 1.54 for the Case II.

Table 1: Masses and widths determined by the χ^2 analysis for the cases I and II.

		case I		case II	
isospin	n	mass (GeV/ c^2)	width (GeV)	mass (GeV/ c^2)	width (GeV)
$I = 1$	1	1.341	0.3221	1.352	0.325
	2	1.379	0.2204	1.370	0.220
	3	1.599	0.2636	1.587	0.264
	4	1.824	0.3679	1.826	0.368
	5	2.048	0.3848	2.100	0.398
$I = 0$	1	0.78256	0.844×10^{-2}	0.78256	0.844×10^{-2}
	2	1.01945	0.426×10^{-2}	1.01945	0.426×10^{-2}
	3	1.212	0.1582	1.206	0.1584
	4	1.437	0.2102	1.440	0.2104
	5	1.505	0.1281	1.510	0.1285

Table 2: The coefficients $a_i^{I,n}$, residues at the resonance poles, determined by the χ^2 analysis for the cases I and II.

		case I		case II	
isospin	n	$a_1^{I,n}$ (GeV 2)	$a_2^{I,n}$ (GeV 2)	$a_1^{I,n}$ (GeV 2)	$a_2^{I,n}$ (GeV 2)
$I = 1$	1	-4.66	8.45	-4.47	8.37
	2	8.489277	-17.50252	7.4739945	-15.8900
	3	-9.623356	13.46278	-8.050218	10.93951
	4	7.065036	-7.310033	6.091668	-6.071918
	5	-0.140	1.36	-0.118	1.11
$I = 0$	1	0.899887	0.02568286	0.8762127	0.09468219
	2	-3.625433	0.5913331	-3.514823	0.3151743
	3	7.385961	-2.033127	6.954618	-1.526721
	4	-3.934473	-1.019970	-3.579443	-2.125879
	5	-1.028184	2.582630	-1.038278	3.394527

Table 3: The coefficients $c_{i,j}^{QCD,I}$ of the QCD terms for the cases I and II determined by the χ^2 analysis.

		case I		
isospin	i	$c_{i,2}^{QCD,I}$	$c_{i,3}^{QCD,I}$	$c_{i,4}^{QCD,I}$
$I = 1$	1	0.5505731	-4.12	-6.50
	2	3.758361	-0.4002×10^2	0.6224×10^2
$I = 0$	1	1.108707	-2.76	-0.7045×10^2
	2	-5.215940	0.6706×10^2	-0.19908×10^3
		case II		
isospin	i	$c_{i,2}^{QCD,I}$	$c_{i,3}^{QCD,I}$	$c_{i,4}^{QCD,I}$
$I = 1$	1	$-0.7186148 \times 10^{-1}$	1.48	-6.99
	2	4.252983	-0.4375×10^2	0.5543×10^2
$I = 0$	1	0.8918455	-1.10	-0.6787000×10^2
	2	-5.617625	0.7029×10^2	-0.19551×10^3

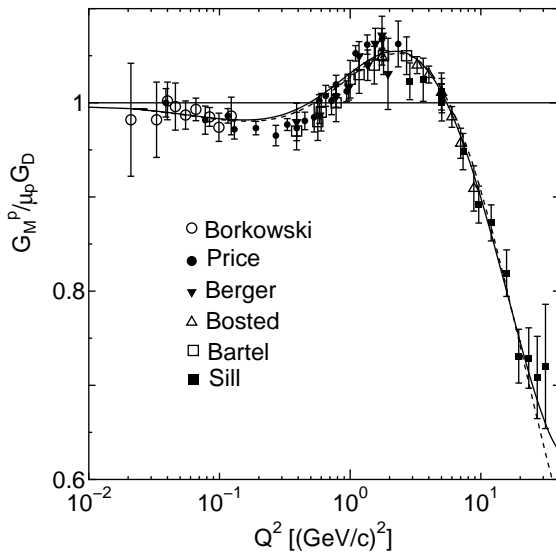


Figure 1: Proton magnetic form factor for the space-like momentum. The solid curve is the result for case I and the dashed one for the case II.

We illustrate in Figs. 1 - 9 the calculated results for the form factors. The results for the Case I is given by the solid curve and Case II by the dashed one. Figs. 1 - 4 the results for the space-like momentum are illustrated: Fig. 1 the proton magnetic form factors $G_M^p/\mu_p G_D$, Fig. 2 proton electric form factor G_E^p/G_D , Fig. 3 the neutron magnetic form factor G_M^n/μ_n and Fig. 4 the neutron electric form factor. In Fig. 5 we illustrate the ratio of proton electric and proton magnetic form factors $\mu_p G_E^p/G_M^p$. We find that $G_E^p = 0$ at $Q^2 = 6.57$ $(\text{GeV}/c)^2$ for the case I and $Q^2 = 6.79$ $(\text{GeV}/c)^2$ for the case II. The form factor for the time-like momentum $|G|$ is given in Fig. 6 for the proton and in Fig. 7 for the neutron. The result for the proton form factor agrees with the experimental data, but for the neutron the calculated one becomes larger than the experiments for large Q^2 .

In Fig. 8 we compare the calculated result for the neutron magnetic form factor $G_M^n/\mu_n G_D$ with the recent experiments. The solid curve agrees with the experimental data very well. The dashed one becomes a little larger than the result obtained by the CLAS collaboration. However, the deviation is not very large. In Fig. 9 we illustrate the result for $|G_E^p/\mu_p G_M^p|$ for the time-like momentum. There seems to be some discrepancy between the experimental data: The ratio obtained by Bardin et al. [8] is smaller than that of Aubert et al. [9]. Our result coincides with the result of Bardin et al. for small Q^2 and that of Aubert et al. for large Q^2 .

5 Concluding Remarks

The experimental data for the neutron magnetic form factor for the space-like momentum with $Q^2 = 1.4 - 4.8$ $(\text{GeV}/c)^2$ [7], mentioned in Sec. 1, are reproduced very well by our calculation.

The absorptive parts of the form factors for the asymptotic region are approximated by the power series in the effective coupling constant of QCD, which begins $O(\alpha_R^2)$ as is given in (36). We have taken three terms in the expansions; the terms of order up to $O(\alpha_R^4)$ are necessary to reproduce the experiments as in the case of deep inelastic electron scattering processes.

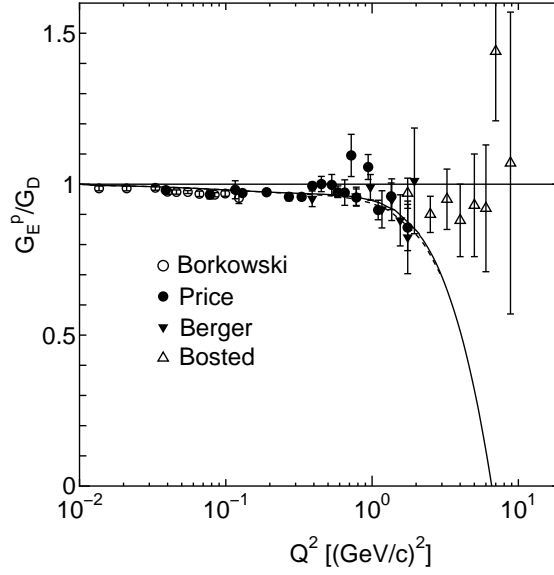


Figure 2: Proton electric form factor for the space-like momentum. The solid curve is the result for case I and the dashed one for the case II.

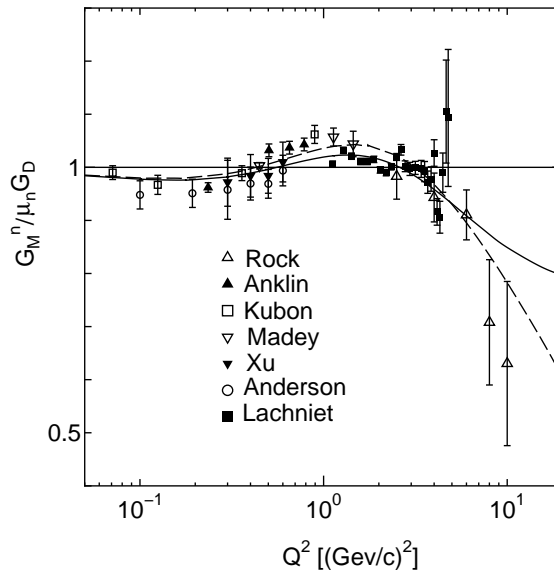


Figure 3: Neutron magnetic form factors for the space-like momentum. The solid curve is the result for case I and the dashed one for the case II.

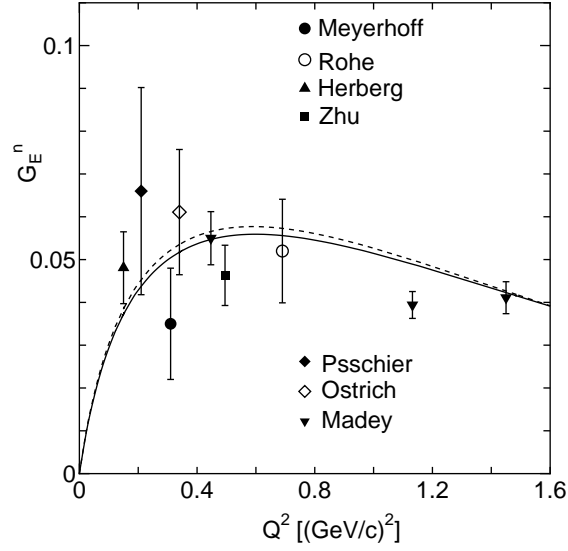


Figure 4: Neutron electric form factor for the space-like momentum. The solid curve is the result for case I and the dashed one for the case II.

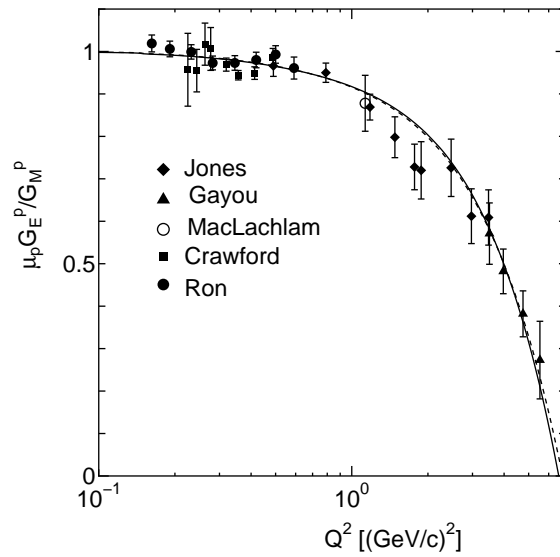


Figure 5: Ratio of the electric and magnetic form factors of proton for the space-like momentum. The solid curve is the result for case I and the dashed one for the case II.

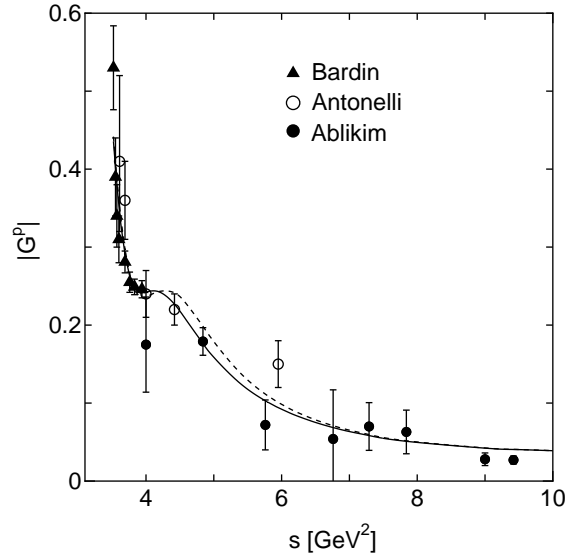


Figure 6: Proton form factors for the time-like momentum. The solid curve is the result for case I and the dashed one for the case II.

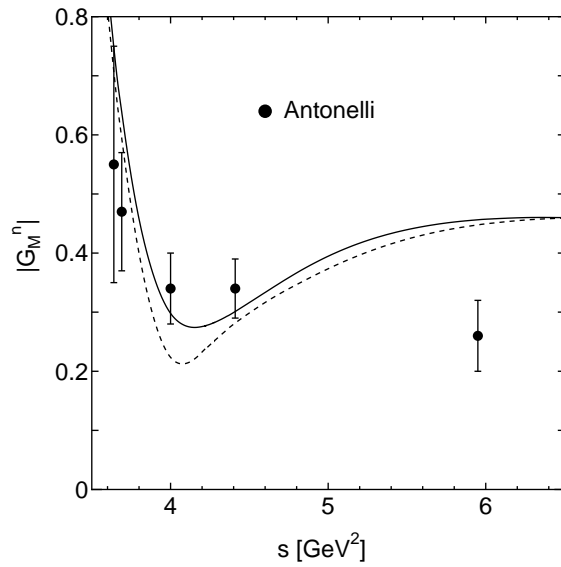


Figure 7: The neutron form factor for the time-like momentum. The solid curve is the result for case I and the dashed one for the case II.

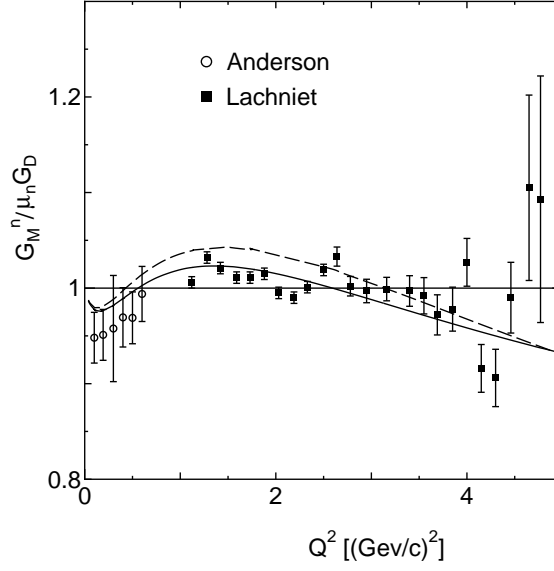


Figure 8: Neutron magnetic form factor for the space-like momentum in the few $(\text{GeV}/c)^2$ region. The solid curve is the result for case I and the dashed one for the case II.

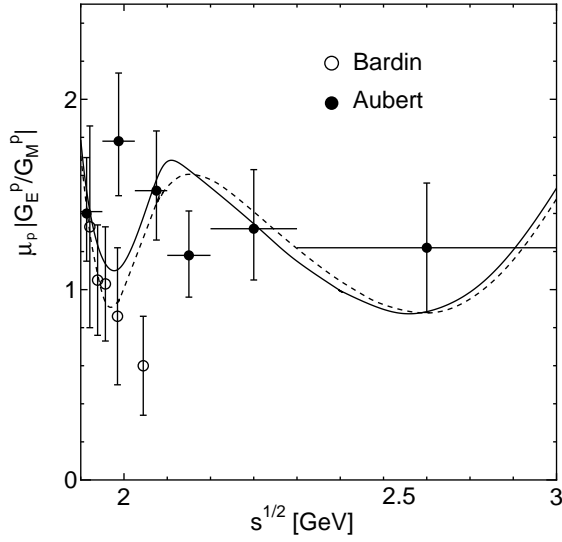


Figure 9: $|G_E^p / \mu_p G_M^p|$ for the time-like momentum. The solid curve is the result for case I and the dashed one for the case II.

It is remarked here that the electromagnetic form factor of bosons, both for the space-like and time-like momenta, can be explained with recourse to the superconvergent dispersion relation with the QCD constraints [18].

For the electric form factor of proton there are deviation of the dispersion theoretical calculation from the experimental data for large Q^2 , where the data were obtained by using the Rosenbluth formula. The discrepancy may imply the necessity of correction of two photon processes to the experimental data [41] [42].

We used the experimental data for the helicity amplitudes obtained by Höher and Schopper in which the contribution from the ρ meson is included. As their data are limited to low t (≤ 0.779 (GeV/c)²), we do not have sufficient data for the region $s \leq 4m_N^2$. We supplemented the unphysical region for $I = 1$ state by introducing vector bosons with the mass, $m_V \lesssim 1.4 \text{ GeV}/c^2$. For the isoscalar state we also introduced a vector boson with the mass about $1.2 \text{ GeV}/c^2$.

In our calculation we treated all of the vector boson masses and widths as parameters. If they are kept at experimental values, we get poor results. The superconvergence conditions are so strong that the value of χ^2 is very sensitive to the mass and width. The masses are obtained to be smaller than the experimental value and the existence of vector bosons with the masses around $1.2 \sim 1.4 \text{ GeV}/c^2$ are necessary both for the $I = 1$ and $I = 0$ states.

To conclude the paper we remark on the mass around $1.2 \text{ GeV}/c^2$. We have introduced the vector boson to supplement the lack of information on the the small Q^2 . However, both for $I = 0$ and $I = 1$ states there are indications of resonances observed by the processes $e^+e^- \rightarrow \eta\pi^+\pi^-$, $\gamma p \rightarrow \omega\pi^0 p$ and $B \rightarrow D^*\omega\pi^-$ [43]. Incorporation of further resonances may improve results for the time-like momentum.

The authors wish to express gratitude to Professor M. Ishida for the valuable discussions and comments. We also would like to thank Dr. T. Komada for the information on the vector bosons with the mass around $1.2 \text{ GeV}/c^2$.

References

- [1] M.K. Jones et al., Phys. Rev. Lett **84**, 1398 (2000).
- [2] O. Gayou et al., Phys. Rev. Lett. **88**, 092301 (2002).
- [3] G. MacLachlan et al., Nucl. Phys. **A764**, 261 (2006).
- [4] C.B. Crawford et al., Phys. Rev. Lett. **98**, 052301 (2007).
- [5] G. Ron et al., Phys. Rev. Lett. **99**, 202002 (2007).
- [6] B. Anderson et al., Phys. Rev. C **75**, 034003 (2007).
- [7] J. Lachniet et al., Phys. Rev. Lett. **102**, 192001 (2009).
- [8] G. Bardin et al., Nucl. Physy. **B411**, 3 (1994).
- [9] B. Aubert et al., Phys. Rev. D **73**, 012005 (2006); hep-ex/0512020.
- [10] S.J. Brodsky and G.R. Farrar, Phys. Rev. Lett. **31**, 1153 (1973); Phys. Rev. D **11**, 1309 (1975); G.P. Lepage and S.J. Brodsky, Phys. Rev. D **22**, 2157 (1980); V.L. Chernyak and I.R. Zhitnitsky Nucl. Phys. **B246**, 52 (1984).
- [11] H. F. Jones and I.L. Solovstov, Phys. Lett. **B349**, 519 (1995).
- [12] Yu.L. Dokshitzer and B.R. Webber, Phys. Lett. **B352**, 451 (1995).
- [13] Yu.L. Dokshitzer, G. Marchesini and B.R. Webber, Nucl. Phys. **B469**, 93 (1996).

- [14] S. Furuichi and K. Watanabe, Prog. Theor. Phys. **82**, 581 (1989); P. Mergell, Ulf-G. Meißner, D. Drechsel, Nucl. Phys. **A596**, 367 (1996).
- [15] M.A. Belushikin, H.-W. Hammer and U.-G.Meissner, Phys. Rev. C **75**, 035202 (2007); hep-ph/0608337.
- [16] G. Höhler and H.H. Schopper, Landolt-Börnstein, I/9b 2, (1983).
- [17] S. Furuichi and K. Watanabe, Prog. Theor. Phys. **92**, 339 (1994).
- [18] M. Nakagawa and K. Watababe, Nouvo Cimento **112 A**, 873 (1999) ; Phys. Rev. C **61**, 055207 (2000); M. Nakagawa, H. Ishikawa and K. Watanabe, Acta Phyica Polonica B **31**, 2539 (2000); arXiv:0809.3334.
- [19] P.E. Bosted et al., Phys. Rev. C **42**, 38 (1990).
- [20] S. Rock et al., Phys. Rev. Lett. **49**, 1139 (1982).
- [21] H. Anklin et al., Phys. Lett. **B428**, 248 (1998).
- [22] M. Meyerhoff et al., Phys. Lett. **B327**, 201 (1994).
- [23] J. Becker et al., Euro. Phys. J. A **6**, 329 (1999).
- [24] C. Herberg et al., Eur. Phys. J A **5**, 131 (1999).
- [25] I. Passchier et al., Phys. Rev. Lett. **82**, 4988 (1999).
- [26] M. Ostrick et al., Phys. Rev. Lett **83**, 276 (1999).
- [27] C. Herberg et al., Eur. Phys. J A **5**, 131 (1999).
- [28] G. Kubon et al., Phys. Lett. **B524**, 26 (2002).
- [29] W. Xu et al., Phys. Rev. C **67**, 012201(R) (2003).
- [30] D. Rohe et al., Phys. Rev. Lett. **83**, 4257 (1999).
- [31] H. Zhu et al., Phys. Rev. Lett. **87**, 081801 (2001).
- [32] M. Ablikim et al., Phys. Lett. **B630**, 14 (2005).
- [33] A. Antonelli et al., Nucl. Phys. **B517**, 3 (1998).
- [34] F. Borkowski et al., Nucl. Phys. **B93**, 461 (1975).
- [35] P.E. Bosted et al., Phys. Rev. Lett. **68**, 3841 (1992).
- [36] Ch. Berger et al., Phys. Lett. **B35**, 87 (1971).
- [37] L.E. Price et al., Phys. Rev. D **4**, 45 (1971).
- [38] W. Bartel et al., Nucl. Phys. **B58**, 429 (1973).
- [39] A.F. Sill et al., Phys. Rev. D **48**, 29 (1993).
- [40] R. Madey et al., Phys. Rev. Lett. **91**, 122002 (2003).
- [41] D. Borisjuk and A. Kobushkin, Phys. Rev. C **76**, 022201(R) (2007).
- [42] M.A. Belushkin, H.-W. Hammer and Ulf-G. Meissner, Phys. Lett. **B658**, 138 (2008).
- [43] On the vector boson with the mass around 1.3 GeV², see T. Komada, hep-ph/0612339, (KEK-Proceedings, P93); W.-M. Yao et al. (Particle Data Group), J. Phys. G **33**, 1 (2006).